Applied Thermal Engineering 201 (2022) 117845

Contents lists available at ScienceDirect

Applied Thermal Engineering

journal homepage: www.elsevier.com/locate/apthermeng

Focusing dielectric slabs for the optimization of heating patterns in single mode microwave applicators

B. García-Baños [a,*], P. Plaza-González [a], J.R. Sánchez [a], S. Steger [b], A. Feigl [b], F. L. Peñaranda-Foix [a], J.M. Catalá-Civera [a]

[a] ITACA Institute, Universitat Politècnica de València, Camino de Vera, 46022 Valencia, Spain
[b] KRONES AG, Böhmerwaldstr. 5, 93073 Neutraubling, Germany

ARTICLE INFO

Keywords:
Dielectric slabs
Microwave heating
Uniformity
Temperature profile
Plastic preform
Heating pattern

ABSTRACT

A new approach based on dielectric slabs with adjustable position is proposed as near-field focusing lenses inside a single-mode microwave applicator to provide specific temperature distributions within a material heated by microwaves.

Numerical and experimental results in a TE_{101} rectangular cavity at 915 MHz have been used to evaluate the capability of these focusing dielectrics to optimize the temperature profile of Polyethylene terephthalate (PET) preforms. Measurements of the temperature profile on the preforms verified the strong effect of the slabs on the electric field distribution, allowing the optimization of the heating patterns with great flexibility.

The successful application applied to PET preforms with different sizes and geometries showed the versatility of this approach which can be extended to the application of other type of loads and microwave cavities.

1. Introduction

Microwave systems are well-known and commonly used in the industry for heating applications, showing clear advantages over more conventional heating technologies, as energy savings, shorter processing time or reduction of environmental impact [1–3]. One of the main features of microwave heating is that the temperature distribution in the processed materials is very dependent on the inherent nature of standing wave patterns of microwaves in the microwave heating chambers, which normally leads to non-uniform volumetric distribution of energy inside the products [1,4–6]. Single mode heating applicators supports only one resonant mode and then the apparition of hot-spots created by standing waves is reduced but the temperature distribution depends on the specific shape of the electric field in these chambers [7].

Heating PET preforms is necessary for the blow molding process which is the most common process for manufacturing containers for packing, transporting and storing drinking liquids and is a good example of an application where microwave technology has shown improvements respect to other technologies, as infrared heating. The microwave heating brings a cylindrical PET preform into a pliable stage before the blow shaping stage, delivering plastic bottles with the appropriate properties. In this process, the preform temperature profile is one of the critical parameters for manufacturing a bottle with the desirable mechanical strength [8–10]. However, the lack of flexibility to generate specific temperature profiles on the preforms might limit the industrial application of the microwave technology in this case [8,9].

Achieving the desired heating uniformity or even more, the synthesis of specific heating patterns in processed materials, is still a real challenge for microwave applicator designers in modern microwave heating systems [5,11]. Numerous methods have been suggested for this purpose, that could be categorized into three groups: i) methods acting on the source, ii) methods acting on the sample, iii) methods employing additional elements.

The first group includes the use of more than one frequency (thus modifying the standing wave patterns) [12,13], microwave cavities with multiple inputs [14], the combination of different heating sources (hybrid heating) [15], the modification of the generator power cycle [2] and the design of special feeding systems (i.e. slotted guides) or antennas [6,16–19]. For example, the recent study [13] presents a method to

Abbreviations: FDTD, Finite Differences in Time Domain; FEM, Finite Element Method; ISM, Industrial, Scientific and Medical; PET, Polyethylene terephthalate; PTFE, Polytetrafluoroethylene; TE, Transversal Electric; TEM, Transversal Electric and Magnetic.

* Corresponding author.
E-mail addresses: beagarba@upvnet.upv.es (B. García-Baños), pedplago@itaca.upv.es (P. Plaza-González), jrsanchez@itaca.upv.es (J.R. Sánchez), sebastian.steger@krones.com (S. Steger), alexander.feigl@krones.com (A. Feigl), fpenaran@dcom.upv.es (F.L. Peñaranda-Foix), jmcatala@dcom.upv.es (J.M. Catalá-Civera).

https://doi.org/10.1016/j.applthermaleng.2021.117845
Received 22 April 2021; Received in revised form 3 November 2021; Accepted 21 November 2021
Available online 24 November 2021

Nomenclature

ρ	Material density (g/m^3)
c_P	Specific heat of the material (J/g°C)
T	Temperature (°C)
T_{sim}	Temperature from simulations (°C)
dT/dt	Heating rate (°C/s)
k_T	Thermal conductivity (W/m°C)
Q_{MW}	Microwave-generated heat (W/m^3)
Q_{LOSS}	Heat losses (W/m^3)
$\varepsilon^{'}$	Dielectric constant (dimensionless)
$\varepsilon^{''}$	Dielectric loss factor (dimensionless)
ε_0	Permittivity of free space (8.854×10^{-12}C/Vm)
$\mu^{'}$	Magnetic constant (H/m)
$\mu^{''}$	Magnetic loss factor (H/m)
μ_0	Permeability of free space ($4\pi \times 10^{-7}$H/m)
f	Frequency (Hz)
E	Electric Field intensity (V/m)
H	Magnetic field intensity (A/m)
P_{MW}	Microwave dissipated power (W)
V	Volume (m^3)
λ	Wavelength (m)
S_{11}	Reflection coefficient
C_f	Proportionality Constant

improve the heating uniformity in a dielectric slab by alternating different frequencies of the source inside a monomode near-cutoff waveguide, leading to dynamical movement of the electric field maxima along the sample. In fast heating processes, the alternation of frequencies needs to be very fast, and the method is limited by the matching speed and the precision of the mechanical tuner that needs to track these frequency changes. In another example ([18]), a monopole antenna is inserted into the sample to increase the energy penetration into the mixture, resulting in more uniform distribution of power density. Whereas this could be a solution for liquid mixtures, it is very complex to apply to solid samples with arbitrary shapes, as it is the case of PET preforms. Another possibility is to place phased array antennas on the walls of a multimode microwave oven as proposed in [20] to synthesize near-field focused patterns. Phased array antennas, however, require complicated feeding networks to distribute the input signal with the appropriate magnitude and phase to each antenna. Leaky-wave antennas are another type of antennas to provide specific heating near-field focused patterns as proposed in [21]. They offer simpler topologies since the focused aperture can be implemented in planar form in the cavity walls and the excitation of the antenna can be integrated with the aperture in the form of a single feeding circuit [20]. Despite this technology is very promising to create focused zones in free space, it is still early to consider in future microwave heating ovens.

In the second group, some works reported specific movement of the sample (turntables, fluidized beds, spouted bed dryers, rotary chambers, conveyor belts, strategic movement) [21,22] or suggested the modification of shape, size or composition of the load [23].

The third group includes those methods proposing additional elements such as the well-known metallic mode stirrers to achieve more uniform electric field distributions [24], active packages (mainly for food) with shields and susceptors [25], or the strategic insertion of metallic [26] or dielectric materials close to the load [27–29]. In [29], the sample is placed inside a quartz reactor with a diameter restriction in the middle section respect to the inlet and outlet sections, in order to intensify the dissipated power along that central zone. This option was shown to be effective for a sample completely filling the reactor cross-section (a zeolite fixed bed) but its applicability is not clear for solid samples with arbitrary shapes (PET preforms with different geometries) partially filling the reactor chamber. In other studies [28,30,31], different procedures were employed to design one or two dielectric layers placed close to a sample to obtain a uniform electric field on the sample. These studies determined the required permittivity for the dielectric elements and suggested that they could be created artificially as composites, which requires very precise material manufacturing and hinders its practical implementation in many cases [30].

In this work, a combination of dielectric slabs with adjustable position to operate as near-field focusing lenses inside a single-mode microwave applicator is proposed to shape the heating pattern of a PET preform. The proposed method is based on the interaction between the electromagnetic waves and the dielectric slabs, that cause their reflection, refraction or diffraction [32] leading to specific heating profiles in the processed objects. This is the first approach allowing to provide not only the required electric field uniformity but also enabling the possibility to obtain pre-defined thermal profiles along the preforms with great accuracy. The fact that proposed slabs are movable and based on well-known and available dielectric materials, is also novel respect to other approaches in the literature, which makes this method very convenient due to its versatility (is able to cope with a wide range of preforms geometries, shapes and very different thermal profile requirements) and very close to its potential industrial application. The validity of this method is demonstrated by numerical and experimental results in a TE_{101} rectangular cavity at 915 MHz, verifying the capability of these focusing dielectrics to optimize the temperature profile on PET preforms of different size.

2. Modelling of the microwave applicator

2.1. Design of the microwave applicator

Fig. 1 shows the schematic of the single-mode microwave applicator designed to heat PET preforms. The applicator consists of a rectangular cavity with inner dimensions of width 250 mm, length 190 mm and height 150 mm, filled with dielectric slabs. The cavity is fed through a Type-N coaxial antenna placed at the center of the bottom wall and oriented parallel to the z axis to excite the TE_{101} electromagnetic mode at 915 MHz, which is a typical frequency for microwave industrial applications.

The geometry of the preform (width of the walls, neck dimensions, length, shape, etc.) determines the main features of the bottle after the blowing process and thus a wide range of sizes and shapes can be found depending on the application. In Fig. 1, the preform (50 g) has a tubular shape with rounded bottom with a total length of 125 mm, and inner and outer diameters of 20 mm and 28 mm respectively. This preform is inserted in the cavity through a hole in the top wall of the cavity with a cut-off cylindrical waveguide section to avoid microwave leakage (48 mm inner diameter, 50 mm length).

The dielectric slabs consist of two stacks of 24 microwave-transparent PTFE (polytetrafluoroethylene) oriented parallel to the y-axis and placed at both sides of the preform. Each slab has a width of 25 mm, a length of 190 mm and a height of 5 mm. The position of each slab in the x-axis determines the distance to the preform and can be individually adjusted providing great flexibility in the positioning of slabs along the preform.

2.2. Microwave heating equations

The mathematical description of microwave heating processes involves simultaneously electromagnetic equations (Maxwell equations)

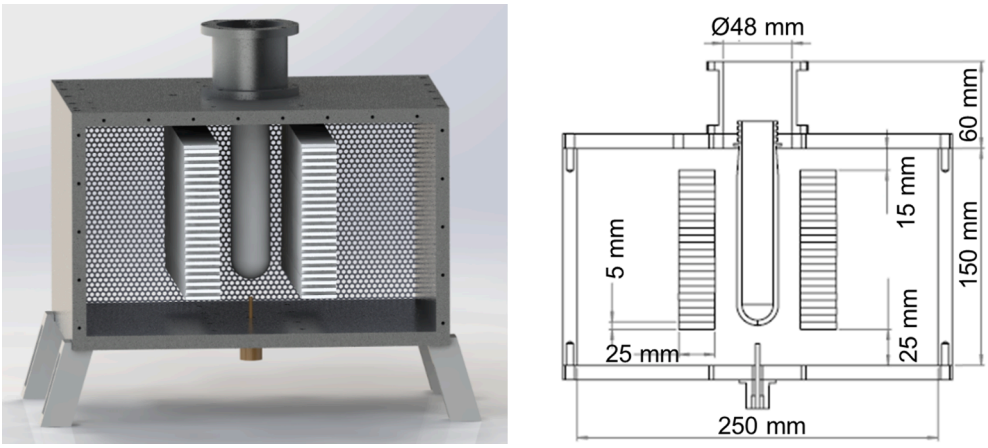

Fig. 1. Design of the microwave cavity with the dielectric slabs and a PET preform.

and heat transfer equations considering temperature-dependent parameters. The Fourier energy balance equation relates the increase of heat in a material with the net inflow of heat, the net production of heat in its volume and the losses of the cavity [33]:

$$\rho c_P \frac{dT}{dt} = \nabla \cdot (k_T \cdot \nabla T) + Q_{MW} - Q_{LOSS} \quad (1)$$

where ρ is the density of the material (g/m^3), c_P is the specific heat of the material (J/g°C), dT/dt is the heating rate (°C/s), k_T is the thermal conductivity, Q_{MW} is the microwave-generated heat in the material (W/m^3), and Q_{LOSS} is any contribution to heat losses in the cavity per unit volume (W/m^3).

The heat generated by microwave energy in the material Q_{MW} (W/m^3) is defined as the microwave power per volume unit and depends on the absorption capability given by the dielectric loss factor ε'' and magnetic loss factor μ'' of the material, the frequency (f) of the microwave excitation (Hz), and the magnitude of the applied Electric (E) and Magnetic (H) fields [33]:

$$Q_{MW} = \frac{P_{MW}}{V} = 2\pi f \varepsilon_0 \varepsilon'' |E|^2 + 2\pi f \mu_0 \mu'' |H|^2 \quad (2)$$

where P_{MW} is the average microwave power (W) dissipated by a sample of volume V(m^3), $\varepsilon_0 = 8.854 \times 10^{-12}$ (C/Vm) and $\mu_0 = 4\pi \times 10^{-7}$ (H/m) are the permittivity and permeability of free space. In the case of PET preforms, the material is non-magnetic in nature ($\mu'' = 0$), and thus the second term of equation (2) can be neglected, being only the dielectric contribution to the heat generation considered in this study.

Assuming that the microwave heating process is fast enough, the effect of thermal conductivity in the sample and the cavity losses can be neglected in (1), and the heating rate mainly depends on the microwave power dissipated in the material. Combining (1) and (2), the temperature profile of the sample is then proportional to the dissipated power profile:

$$\rho c_P \frac{dT}{dt} \approx P_{MW} \quad (3)$$

Therefore, according to (3), the electric field or the microwave dissipated power distribution in the microwave applicator can provide a good estimation of the temperature profile along the PET preform. This means that the electromagnetic simulation providing the dissipated power profile (only dependent on the dielectric properties) is giving enough information to know the temperature profile and there is no need to compute the left side of equation (3). Thus, the thermal properties of PET (c_P = 1.2 J/g°C, k_T=0.146 W/m°C) are not needed in the model. The proportionality that relates the dissipated power and the resulting temperature will be empirically adjusted in the measurements section.

The electric field distribution in a microwave cavity is determined by solving the Maxwell equations according to a specific excitation and the boundary condition imposed by the applicator geometry. Applicators with simple geometries such empty single mode resonant cavities can be studied analytically [11,12,30], but when these structures include complex shapes with dielectrics partially filling the cavity, the use of analytic methods is very limited [1,34]. Then, the solution of Maxwell equations in three dimensions of complex geometries and different material properties, as the geometry illustrated in Fig. 1, requires the use of numerical modelling techniques.

During last years, the advent of powerful computational resources has led to the fast development of different numerical techniques for solving Maxwell equations in complex geometries. Finite Element Method (FEM) and Finite Difference in Time Domain method (FDTD) are examples widely employed by many electromagnetic solvers for these purposes. In general, it is well accepted the ability of FEM to model complex geometries and the computational efficiency of FDTD calculating the response of the system over a wide range of frequencies with a single simulation [35].

2.3. Electromagnetic modelling

Electromagnetic fields in the microwave applicator were numerically solved with the aid of the Quickwave 3D (QW3D) Simulator (QWED, Poland) [36]. QW3D allows to define the geometry of Fig. 1 and run a FDTD analysis with a specific sinusoidal excitation to calculate the electric field distribution in the cavity and the S_{11} parameter (reflection coefficient) in a frequency range.

Fig. 2 shows the electromagnetic model of the single-mode applicator developed in the QW3D graphic editor surrounded by the appropriate boundary conditions. A perfect electrical conductor boundary condition was defined for the microwave cavity walls and the conductors of the input coaxial antenna. To complete the model, the permittivity of PTFE elements (ε_r = 2.06-j0.0001), and PET preform (ε_r = 2.6-j0.025) were measured with the methods described in [37,38] respectively and these values were introduced in the software. A variable mesh size was applied in the model, to increase the simulation accuracy in those zones with more complex geometry variations, enforcing an average cell size of $\lambda_{min}/10$, where λ_{min} stands for the wavelength at the largest frequency of interest, namely, f = 1 GHz, in the material with the highest dielectric constant (PET preform). This value of $\lambda_{min}/10$ was suggested as appropriate to obtain a good balance between accuracy and computational time in previous mesh studies [27,39].

To verify the performance of the modelling tool, the single-mode cavity model illustrated in Fig. 2 was simulated without the dielectric slabs. The single-mode cavity was excited by a TEM mode through the

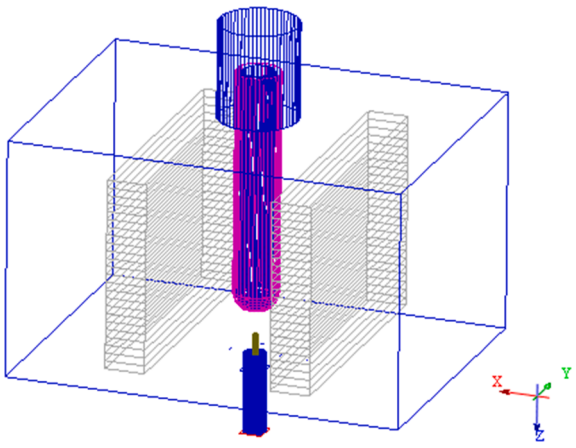

Fig. 2. Electromagentic model of the microwave cavity with the preform and dielectric slabs.

coaxial antenna and 1 W of power. The simulation work was carried out on a computer with Intel Core i7-8700, 3.20 GHz processor with 16 GB RAM memory and 64 bit Windows 10 enterprise operating system.

Fig. 3 shows the results of magnitude of the reflection coefficient $|S_{11}|$ as a function of the frequency, the distribution of electric field at the resonance peak and the dissipated power in the PET preform. The mean computational time was about 1 min for the $|S_{11}|$ and about 5 min for the electric field and power distributions.

Electromagnetic field patterns of Fig. 3b and Fig. 3c show the field distribution of the TE_{101} mode in the rectangular cavity with uniformity in height and maximum in the center where the PET sample is located. However, the dissipated power distribution (Fig. 3d) along the PET preform is not uniform because the preform locally modifies this nominal electric field, making it more enhanced in the middle part and lower at both extremes. Fig. 3d also shows the attenuation of fields in the cut-off hole at the top avoiding the heating of the preform parts at this position and any microwave leakage out of the applicator.

The effect of the dielectric slabs is presented in Fig. 4. The position of the slabs has been chosen for illustrative purposes. The presence of the slabs increases the dielectric load in the cavity, thus shifting the resonance frequency to lower values (Fig. 4.a). Electromagnetic field patterns (Fig. 4b and Fig. 4c) show how the field distribution of the TE_{101} mode is strongly affected by the slabs, specially by those located closer to the center. In this case, the electric field maximum is redistributed around the slabs and the field strength on the preform is decreased at that zone. The effect of the slabs which are closer to the preform is then observed as a "valley" in the dissipated power profile (Fig. 4d), whereas it is enhanced just above and below these slabs due to their edge effect.

3. Experimental set-up

To verify the proposed approach, a complete microwave system was developed to heat the PET preforms and measure the thermal profile of

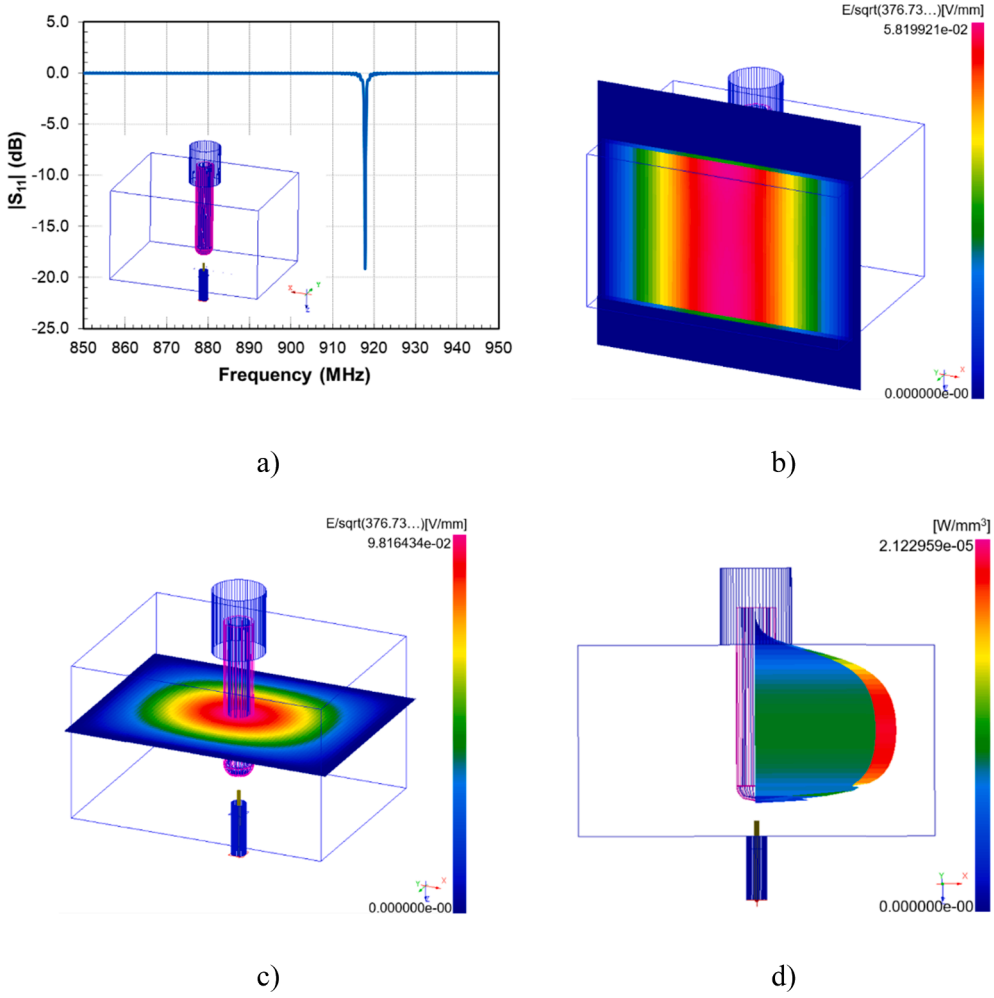

Fig. 3. Simulations/Modelling of the cavity without slabs. a) $|S_{11}|$ as a function of frequency, b) Electric field distribution (XY plane), c) Electric field distribution (XZ plane), d) Dissipated power in the preform.

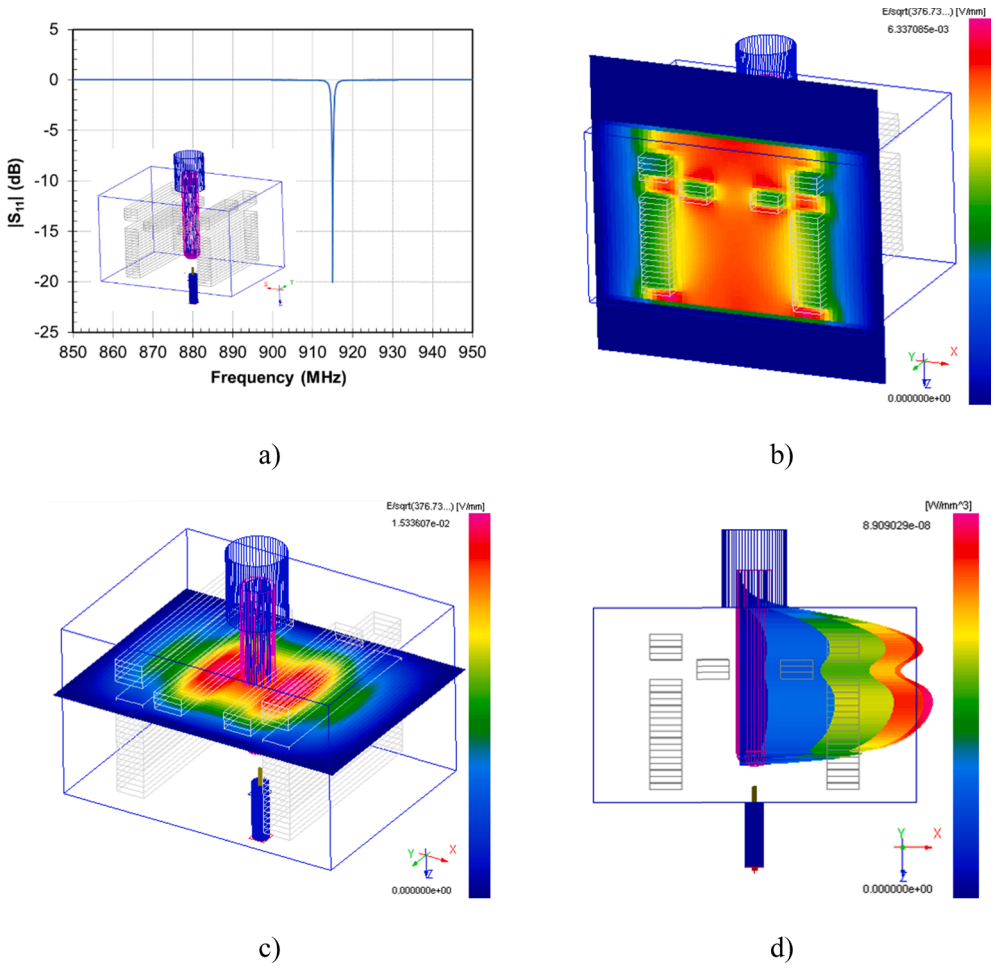

Fig. 4. Simulations/Modelling of the cavity with slabs at certain position. a) $|S_{11}|$ as a function of frequency, b) Electric field distribution (XY plane), c) Electric field distribution (XZ plane), d) Dissipated power in the preform.

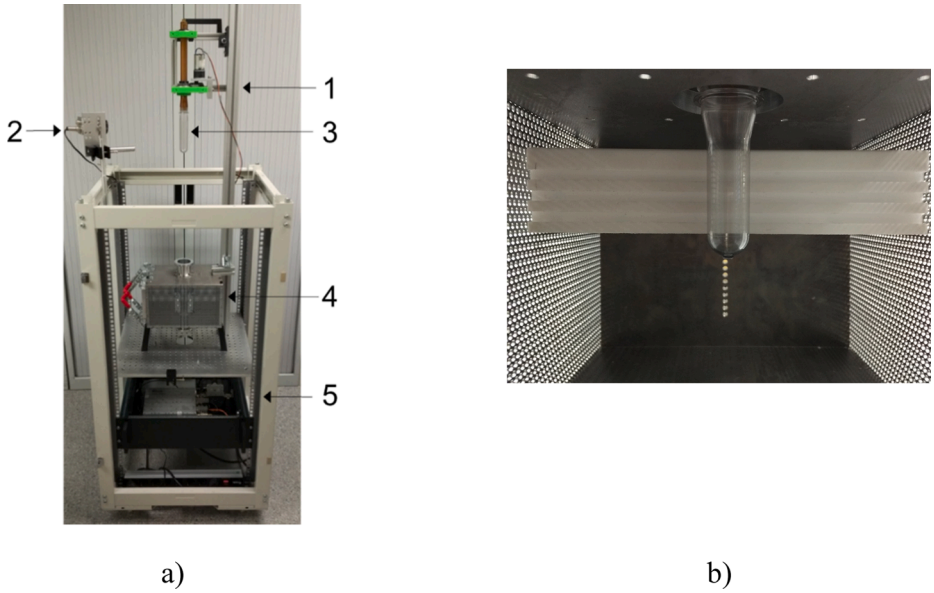

Fig 5. Experimental setup. a) Microwave system (1. Vertical displacement and rotation device, 2. Thermal camera, 3. PET preform, 4. TE_{101} cavity, 5. Solid state generator). b) Example of a preform with PTFE slabs in the TE_{101} cavity.

the samples (Fig. 5a).

The single-mode TE_{101} rectangular microwave cavity with PTFE slabs was manufactured according to the schematic of Fig. 1. Two of the cavity walls were manufactured with metal grids for inspection from outside and to hold the PTFE slabs with the possibility to individually adjust their distance to the preform (see Fig. 5b).

Two thermal cameras (PI-160, Optris GmbH) were employed for temperature measurements. One was positioned in front of the applicator to control the PET preform temperature through the metal grid. The second camera was placed above the applicator for accurate temperature profile measurements once the preform was removed from the applicator after the heating process. The preform was inserted from the top hole attached to a vertical displacing device that allowed a fast movement to the specific position into the cavity and back to the initial position in front of the thermal camera. It is important to note that profile measurements were recorded in less than 1 s after the heating period, since 2 s was determined as the limit to avoid the influence of subsequent diffusion and cooling processes taking place in the preform. This device also includes a turning drive that rotates the preform to ensure rotational symmetry in the thermal profile.

Both thermal cameras were calibrated to factory specifications, and the emissivity of PET was carefully determined before the experiments. With the aid of a thermocouple in contact with the preform, the emissivity of the cameras was adjusted to provide the real temperature. This procedure was performed at 70 °C [40] with several preforms of two different sizes (50 g and 14 g) and geometries and the mean emissivity value obtained was 0.92, which is in the range of the typical emissivity values of PET preforms found in the literature [40].

A 600 W solid state generator (GLS600, Sairem) around the ISM frequency of 915 MHz (from 900 MHz to 920 MHz) was selected to feed the microwave applicator through the coaxial antenna placed vertically to excite the TE_{101} mode.

The heating process was divided in two steps. In the first step there was a fast sweep of frequencies in the generator from 900 to 920 MHz at low power to identify the resonant frequency of the cavity (the frequency providing the lowest value of reflection $|S_{11}|$, see Fig. 3.a) or 4. a)). In the second step this single frequency was fixed in the generator with the maximum power (600 W) to reach the desired temperature in the preform in the shortest time period. The maximum temperature was controlled through the grid with the first thermal camera to avoid overheating of the sample. After the selected heating time, the preform was quickly removed from the applicator and positioned in front of the second thermal camera for accurate temperature profile measurements. A heating period of 20 s was selected for the experiments with 50 g preforms, and a heating period of only 7 s was selected for the 14 g preforms because it provided a final maximum temperature in the preforms close to 100 °C, which avoids PET crystallization and is in accordance to the requirements of the subsequent blowing step in the real industrial process.

4. Measurements

To evaluate the performance of the proposed approach, several scenarios were considered and the effect of the dielectric slabs in the single-mode microwave applicator was quantified through temperature measurements of the PET preforms, comparing the results with the simulation model described in previous section.

4.1. Microwave applicator without dielectric inserts

The first configuration tested in the microwave system (Fig. 5a) was the heating of a 50 g PET preform in the single-mode applicator without dielectric slabs. After adjustment of the generator frequency (918.9 MHz for minimum S_{11}), the PET preform was processed at maximum power (600 W) during 20 s to reach an approximate temperature of 100 °C, and the thermal profile was measured by the camera after moving the preform outside the microwave cavity.

Fig. 6 illustrates the thermal profile measured along the PET preform. The measured pattern showed temperature values ranging from 40 to 50 °C in the extremes to approx. 100 °C around the middle. Despite the uniformity of the TE_{101} electric field distribution in height (z-axis), the presence of the dielectric PET preform caused a distortion in the cavity fields due to combination of different effects: diffraction, decrease of electric field magnitude inside the material, concentration of electric field near the edges, etc. Therefore, the dissipated power in the preform resulted in less warming within the top and bottom regions compared to the central region.

The estimation of the temperature profile according to the simulated dissipated power in the cavity is also represented in Fig. 6a for comparison purposes. It should be noted here that, according to the explanation given after eq. (3), the estimated temperature (T_{sim}) obtained from the simulated dissipated power was normalized and scaled with a certain constant to be comparable to the measured temperature values as follows:

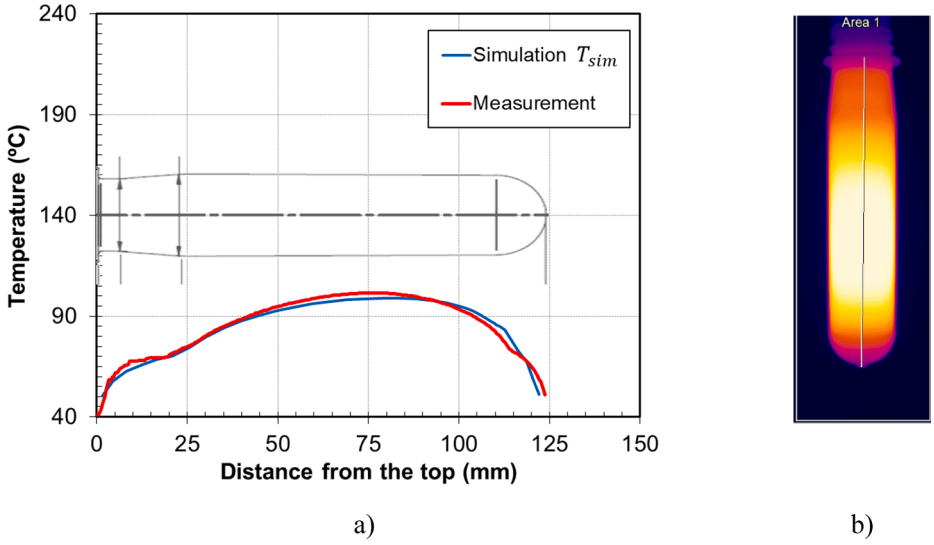

Fig. 6. Thermal profile along the 50 g PET preform in the single mode microwave cavity without dielectric slabs. a) Measured temperature profile compared to simulated temperature profile. b) Thermal image from the lateral IR camera.

$$T_{sim} = \frac{P_{MW}}{P_{MW\,max}} \bullet C_f \quad (4)$$

where P_{MW} is the simulated dissipated power profile and C_f is a constant employed to represent around the values of measured thermal profile.

As Fig. 6a shows, there is a very good agreement between measured and simulated profiles. The small differences between both representations can be attributed to the small uncertainty in the dimensions of the electromagnetic model respect to the real size of the PET preform, especially in those zones with variable wall thickness, and to the thermal diffusion of the preform in the experimental setup, not accounted for in the electromagnetic model.

4.2. Cavity with dielectric slabs

To analyze the possibilities to modify the default temperature pattern of Fig. 6, the PTFE slabs were placed in the microwave cavity at opposite sides of the PET preform, according to the distribution depicted in Fig. 7a. The figure shows 16 slabs close to the preform at a distance of 18 mm from the cavity center and 8 slabs far from the preform at 65 mm from the cavity center (only one side of slabs is shown in Fig. 7.a). Following the same two-step procedure, a 50 g preform was processed during 20 s at 600 W of microwave power (909.3 MHz) and the resulting thermal profile is also presented in Fig. 7.

In this scenario, the presence of the dielectrics reduces the electric field distribution around its position and, as consequence, the temperature at the preform extremes (90–106 °C) was enhanced respect to temperature at the central zone (70–80 °C). The temperature profile measured by the thermal camera showed then an inverted pattern respect to the temperature distribution of Fig. 6 with overexposed regions out of the dielectric slabs. This can be seen as the slabs "focusing" the energy on the extremes of the preform in contrast to the default profile. Again, the estimation of the temperature profile according to the QW3D simulation of this configuration agrees very well with experimental measurements.

After demonstrating the validity of PTFE dielectric inserts to modify the heating distribution of the PET preform, the next scenario consists of modifying the position of slabs to achieve a specific reference heating profile in the 50 g PET preform according to the mechanical requirements of the subsequent blowing process of the bottle.

Numerous configurations of slabs were simulated with the QW3D model to find the positioning of PTFE that better provides the reference temperature distribution. Fig. 8 shows the simulated estimation of temperature profile compared to the requirement (black line). The reference indicates a steep temperature increase (3–5 °C/mm) at the top of the preform (neck), while the body should have a uniform profile (±4°C). A gradual decrease of temperature was required at the rounded part of the preform.

Fig. 8 also depicts the empirical validation of the temperature profile measured by the thermal camera after 20 s at 600 W (905.8 MHz). As in previous cases, the small differences between simulations and measurements of temperature are attributed to the limitations of the electromagnetic model for areas of variable wall thickness and to the thermal diffusion phenomena.

The slabs placed along the preform body (from the 5th to the 20th) had a "push" effect on the electric field towards the top and bottom of the preform, avoiding the default overheating of the central zone, but maintaining the required uniformity ($\leq \pm 4$°C). The first dielectric slabs were adjusted so that the combined edge effect together with the increase of electric field compensated the default underexposure of the top zone, and at the same time provided the steep temperature slope (4.3 °C/mm), without overheating of the neck at the top (52 °C).

To further illustrate the flexibility of this approach, an example of a preform with very different size and geometry is also reported. Fig. 9 shows a smaller PET preform of 14 g together to the reference temperature profile recommended for this size (black line). The reference temperature was very similar to the previous preform, with a steep increase of the temperature below the neck (3–5 °C/mm), followed by a uniform profile (±4°C) along the body.

The QW3D simulation tool was employed also here to determine the position of slabs that better provides the desired temperature distribution. The overexposure of the central zone was avoided by placing a set of slabs uniformly close to the preform, which pushed the electric field to the top (3.3 °C/mm) and bottom of the preform, thus compensating the default temperature profile imposed by the TE_{101} mode.

The temperature profile was also validated empirically. After the adjustment of the generator frequency (907 MHz), this preform required only 7 s at 600 W to reach the desired temperature (approx. 100 °C). The thermal profile measured by the lateral camera is also shown in Fig. 9.

Once again, the appropriate configuration of the dielectrics set in the microwave cavity was able to re-shape the electric field distribution to achieve the desired temperature pattern on the PET preform.

As expected, the different studied configurations showed different resonance frequencies due to the presence of the slabs and their different

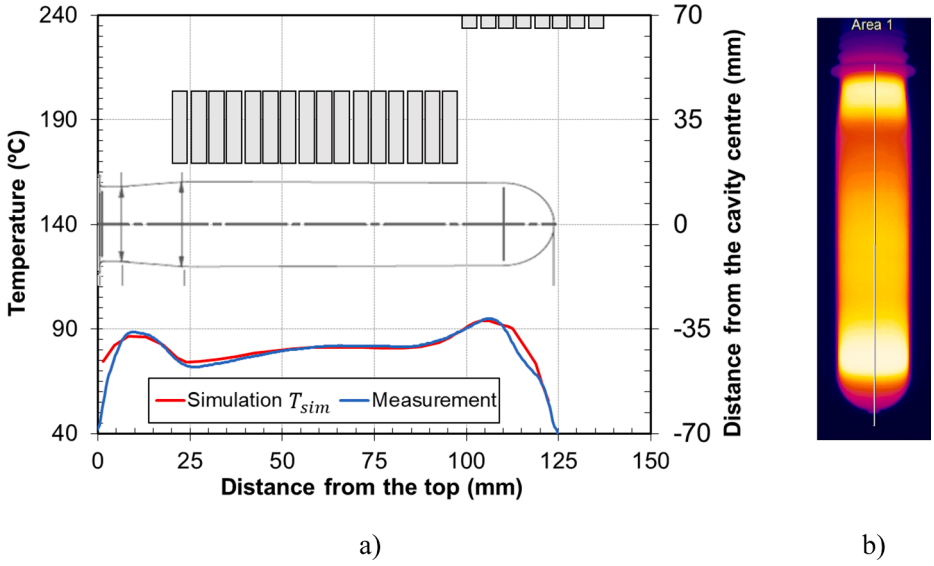

Fig. 7. Thermal profile along the 50 g PET preform with a group of slabs placed at constant distance from the cavity center (only one side of slabs is visible). a) Measured temperature profile compared to simulated temperature profile. b) Thermal image from the lateral IR camera.

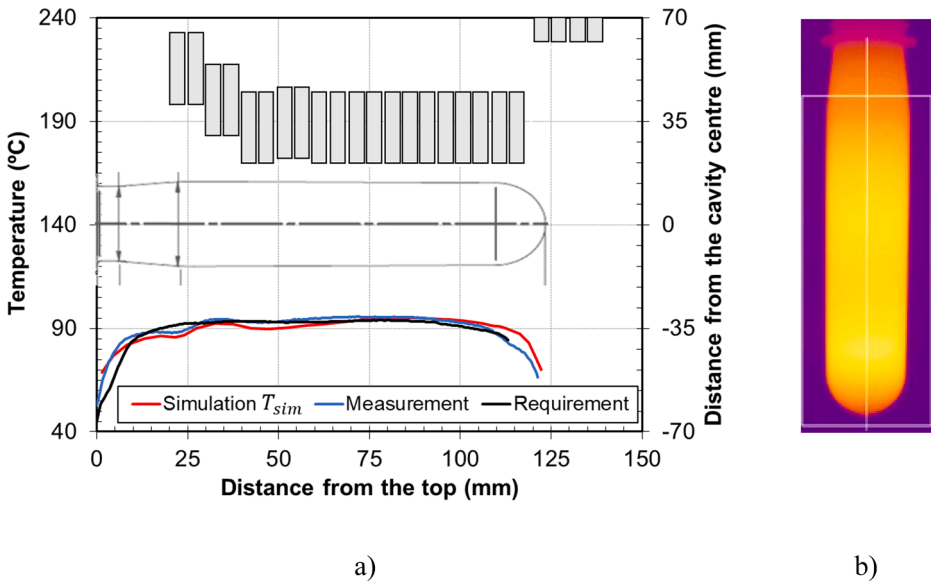

Fig. 8. Thermal profile along the 50 g PET preform with the optimum position of dielectric slabs. a) Measured temperature profile compared to simulated temperature profile and real temperature requirement. b) Thermal image from the lateral IR camera.

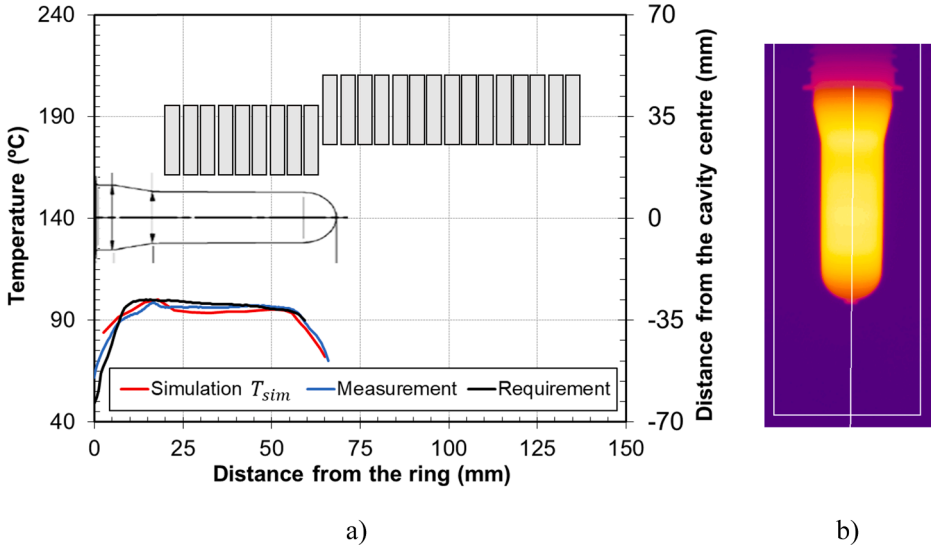

Fig. 9. Thermal profile along the 14 g PET preform with the optimum position of dielectric slabs. a) Measured temperature profile compared to simulated temperature profile and real temperature requirement. b) Thermal image from the lateral IR camera.

positioning. Fig. 10 shows the scattering parameter $|S_{11}|$ as a function of frequency measured with a Vector Network Analyzer to illustrate this effect on the resonance frequency. It should be remarked here as well that, in the case of small preforms (14 g), those slabs that are far away from the preform and have small or negligible influence on the thermal profile, (i.e. the lowest 15 slabs in Fig. 9), may still be used to compensate the increase of the resonance frequency due to the smaller quantity of PET inside the cavity providing an additional procedure to tune the microwave cavity at the frequency of the source close to 915 MHz.

4.3. Error analysis and repetitivity

Different error sources can contribute to the small differences between the predicted and measured temperature profiles: i) non-ideal modelling, ii) non-ideal manufacturing of the preforms, iii) non-ideal experimental settings. An extensive measurement campaign was performed with different slabs configurations and preform sizes, and the mean and maximum error values were obtained. Fig. 11.a) shows the results for 50 g and 14 g preforms. The model was able to predict very accurately (mean error below 5%, maximum error below 6%) the thermal profile along the straight part of the preforms, whereas the error slightly increases at both extremes of the preform (mean error below 8%, maximum error below 11%). One reason is that the model of the preform does not reproduce exactly the geometry of the preforms, which for example presents variations of the wall thickness in the upper and lower extremes. Another reason is that, despite of the fact that the heating process is fast, there may be already some thermal processes taking place (i.e. preferential local cooling of the extremes respect to the central part) that were not considered in the electromagnetic model. An updated model with a more realistic geometry of the preform, would lead to longer computational time but would provide lower discrepancies in the preform extremes.

The reproducibility of the results was also evaluated through

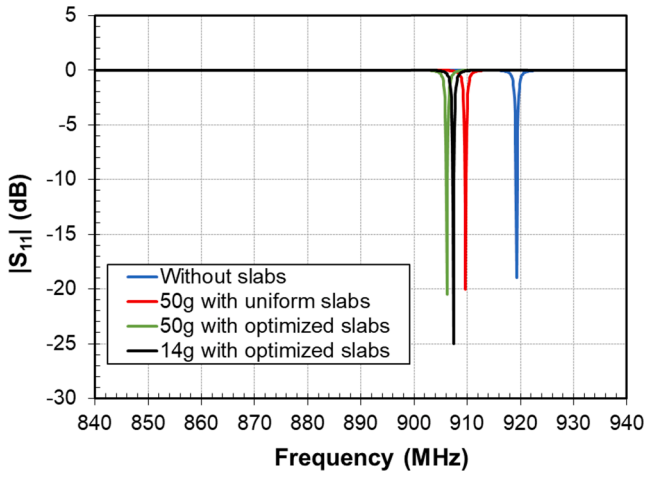

Fig. 10. Scattering parameter $|S_{11}|$ as a function of frequency measured with a Vector Network Analyzer for the different studied configurations.

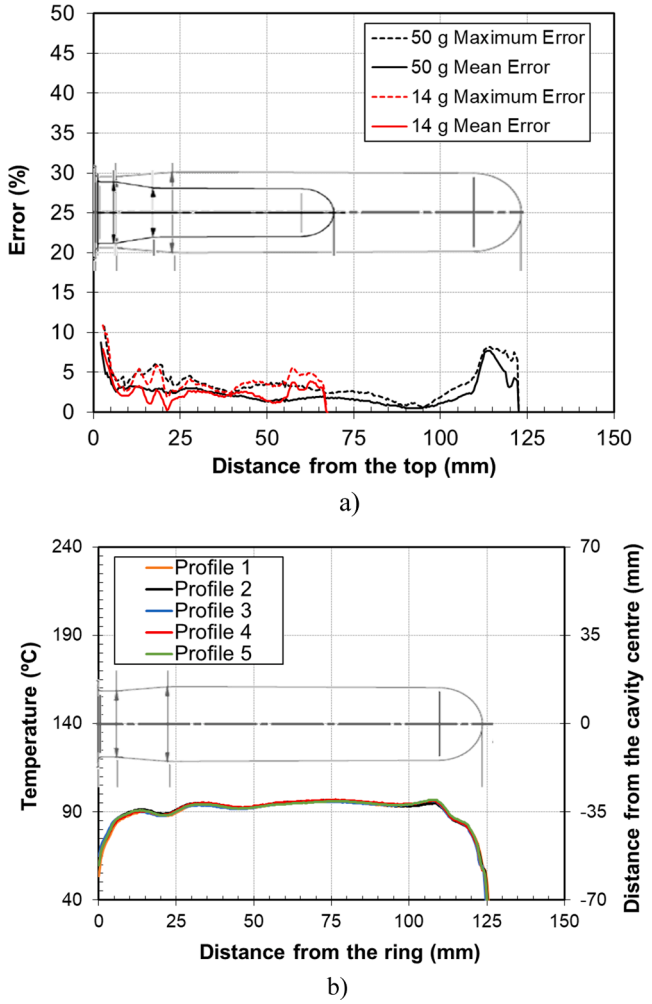

Fig. 11. Error and repetitivity analysis a) Mean and maximum error between predicted and measured thermal profiles, b) Example of repetitivity tests.

different sets of experiments with the same settings. Fig. 11.b) illustrates the repetitivity with an example of 5 measurements of 50 g preforms. The good reproducibility of the results was verified, with temperature differences below 2 °C between measurements. These variations can be attributed to small differences between preforms from the same batch, or small inaccuracies in the positioning of the preform or the slabs.

5. Conclusions

In this work, a combination of dielectric slabs with adjustable position has been proposed to operate as near-field focusing elements inside a single-mode microwave applicator and re-shape the temperature profile of objects under microwave heating.

The processing of PET preforms was selected as an example of application requiring specific temperature profiles and enough flexibility to cope with a wide range of sizes and geometries.

The numerical model allowed accurate predictions of the dissipated power on the preforms, enabling the study of different configurations of the dielectric slabs to strategically develop the required temperature patterns.

The remarkable effect of the dielectric slabs was demonstrated through a set of experiments, where the ability to modify the electric field distribution proved to be particularly useful for generating the desired heating patterns. It should be noted that, in the case that the slabs could be moved dynamically (i.e. by mechanical means), the profile adjustment would be possible in real time.

The proposed concept could be extended to other microwave cavities, tailoring the temperature profile to different types of loads with specific local temperature requirements.

CRediT authorship contribution statement

B. García-Baños: Methodology, Validation, Writing – original draft. **P. Plaza-González:** Software, Investigation. **J.R. Sánchez:** Software, Investigation. **S. Steger:** Resources, Writing – review & editing. **A. Feigl:** Resources, Investigation. **F.L. Peñaranda-Foix:** . **J.M. Catalá.Civera:** Conceptualization, Supervision.

Declaration of Competing Interest

The authors declare that they have no known competing financial interests or personal relationships that could have appeared to influence the work reported in this paper.

Acknowledgments

The authors wish to thank Konrad Senn and Johann Zimmerer for their support, fruitful discussions and useful advice.

References

[1] A.A. Salema, M.T. Afzal, Numerical simulation of heating behaviour in biomass bed and pellets under multimode microwave system, Int. J. Therm. Sci. 91 (2015) 12–24.
[2] L.A. Campañone, J.A. Bava, R.H. Mascheroni, Modeling and process simulation of controlled microwave heating of foods by using of the resonance phenomenon, Appl. Therm. Eng. 73 (1) (2014) 914–923.
[3] J. Ye, C. Zhang, H. Zhu, A temperature-control system for continuous-flow microwave heating using a magnetron as microwave source, IEEE Access 8 (2020) 44391–44399, https://doi.org/10.1109/ACCESS.2020.2978124.
[4] G.S.J. Sturm, M.D. Verweij, T. van Gerven, A.I. Stankiewicz, G.D. Stefanidis, On the effect of resonant microwave fields on temperature distribution in time and space, Int. J. Heat Mass Transf. 55 (2012) 3800–3811.
[5] S.S.R. Geedipalli, V. Rakesh, A.K. Datta, Modeling the heating uniformity contributed by a rotating turntable in microwave ovens, J. Food Eng. 82 (3) (2007) 359–368.
[6] J. Zhang, Y. Luo, C. Liao, F. Xiong, X.i. Li, L. Sun, X. Li, Theoretical investigation of temperature distribution uniformity in wood during microwave drying in three-port feeding circular resonant cavity, Drying Technol. 35 (4) (2017) 409–416, https://doi.org/10.1080/07373937.2016.1178141.

[7] V. Palma, D. Barba, M. Cortese, M. Martino, S. Renda, E. Meloni, Microwaves and heterogeneous catalysis: a review on selected catalytic processes, Catalysts. 10 (2) (2020) 246, https://doi.org/10.3390/catal10020246.

[8] D.U. Erbulut, S.H. Masood, H. Senko, K. Davies, Preheating of a poly(ethylene terephthalate) preform for stretch blow molding using microwaves, J. Appl. Polym. Sci. 112 (2009) 1670–1679, https://doi.org/10.1002/app.

[9] P. Lebaudy, L. Estel, A. Ledoux, Microwave heating of poly(ethylene terephthalate) bottle preforms used in the thermoforming process, J. Appl. Polym. Sci. 108 (2008) 2408–2414, https://doi.org/10.1002/app.27763.

[10] Christian Hopmann, Benjamin Twardowski, Preform heating methods in the two stage stretch blow moulding process, comPETence magazine, ONE:18.

[11] S. Farag, A. Sobhy, C. Akyel, J. Doucet, J. Chaouki, Temperature profile prediction within selected materials heated by microwaves at 2.45GHz, Appl. Therm. Eng. 36 (2012) 360–369.

[12] Z. Du, Z. Wu, W. Gan, G. Liu, X. Zhang, J. Liu, B. Zeng, Multi-physics modeling and process simulation for a frequency-shifted solid-state source microwave oven, IEEE Access 7 (2019) 184726–184733.

[13] S. Jung, J.H. Kwak, S.M. Han, Guided-wavelength-controlled dynamic microwave heating in a near-cutoff waveguide, Appl. Therm. Eng. 188 (2021) 116630, https://doi.org/10.1016/j.applthermaleng.2021.116630.

[14] G. Xiong, H. Zhu, K. Huang, Y. Yang, Z. Fan, J. Ye, The impact of pins on dual-port microwave heating uniformity and efficiency with dual frequency, J. Microw. Power Electromagn. Energy. 54 (2) (2020) 83–98, https://doi.org/10.1080/08327823.2020.1755481.

[15] L. Malafronte, G. Lamberti, A.A. Barba, B. Raaholt, E. Holtz, L. Ahrné, Combined convective and microwave assisted drying: experiments and modelling, J. Food Eng. 112 (2012) 304–312.

[16] Dharmendra-Singh Rajpurohit, Rahul Chhibber, Design optimization of two input multimode applicator for efficient microwave heating, Int. J. Adv. Microwave Technol. (IJAMT) 1 (3) (2016).

[17] H. Giddens, Y. Hao, Multibeam graded dielectric lens antenna from multimaterial 3D printing, IEEE Trans. Antennas Propag. 68 (9) (2020) 6832–6837.

[18] A.A. Dundas, A.L. Hook, M.R. Alexander, S.W. Kingman, G. Dimitrakis, D.J. Irvine, Methodology for the synthesis of methacrylate monomers using designed single mode microwave applicators, React. Chem. Eng. 4 (8) (2019) 1472–1476.

[19] S. Tiefeng, L. Kaldi, High-power solid-state oscillator for microwave oven applications, in: IEEE/MTT-S International Microwave Symposium, 2012.

[20] J.L.G. Tornero, A.P. García, J.M. Cabrera, Microwave heating pattern beamforming using a cylindrical phased-array of antennas. 3rd Global Congress on Microwave Energy Applications, 2016.

[21] S.-H. Bae, M.-G. Jeong, J.-H. Kim, W.-S. Lee, A continuous power-controlled microwave belt drier improving heating uniformity, IEEE Microwave Wirel. Compon. Lett. 27 (5) (2017) 527–529.

[22] J.L. Pedreño-Molina, J. Monzó-Cabrera, J.M. Catalá-Civera, Sample movement optimization for uniform heating in microwave heating ovens, Int. J. RF Microwave Computer-Aided Eng. (2006) 142–152, https://doi.org/10.1002/mmce.

[23] Z. Zhang, T. Su, S. Zhang, Shape effect on the temperature field during microwave heating process, J. Food Qual. 2018 (2018) 1–24.

[24] P. Plaza-Gonzalez, J. Monzo-Cabrera, J.M. Catala-Civera, D. Sanchez-Hernandez, Effect of mode-stirrer configurations on dielectric heating performance in multimode microwave applicators, IEEE Trans. Microw. Theory Tech. 53 (5) (2005) 1699–1706.

[25] ChunFang Song, ShuguangWang YanWang, ZhengWei Cui, Xu Yanfeng, Haiqing Zhu, Non-uniformity investigation in a combined thermal and microwave drying of silica gel, Appl. Therm. Eng. 98 (2016) 872–879.

[26] M. Tao, F. Yang, Z. Tang, J. He, Y. Liao, Periodical metal cylinders for improving heating uniformity of small batch materials in microwave applicators with rotating turntables, Eur. Phys. J. Appl. Phys. 83 (3) (2018) 30901, https://doi.org/10.1051/epjap/2018180054.

[27] J. Wang, T. Hong, T. Xie, F. Yang, H.u. Yusong, H. Zhu, Impact of filled materials on the heating uniformity and safety of microwave heating solid stack materials, Processes 6 (2018) 220, https://doi.org/10.3390/pr6110220.

[28] J.T. Bernhard, W.T. Joines, Dielectric slab-loaded resonant cavity for applications requiring enhanced field uniformity, IEEE Trans. Microwave Theory Techn. 44 (3) (1996) 457–460.

[29] E. Meloni, M. Martino, P. Pullumbi, F. Brandani, V. Palma, Intensification of TSA processes using a microwave-assisted regeneration step, Chem. Eng. Process. - Process Intens. 160 (2021) 108291, https://doi.org/10.1016/j.cep.2020.108291.

[30] E. Dominguez-Tortajada, J. Monzo-Cabrera, A. Diaz-Morcillo, Uniform electric field distribution in microwave heating applicators by means of genetic algorithms optimization of dielectric multilayer structures, IEEE Trans. Microw. Theory Tech. 55 (1) (2007) 85–91.

[31] K.A. Laurie, V.V. Yakovlev, Method of control and optimization of microwave heating in waveguide systems, IEEE Trans. Magn. 35 (3) (1999) 1777–1780.

[32] J. Baker-Jarvis, S. Kim, The interaction of radio-frequency fields with dielectric materials at macroscopic to mesoscopic scales, J. Res. Natl. Inst. Stand Technol. 117 (2012) 1, https://doi.org/10.6028/jres10.6028/jres.117.001.

[33] R.R. Mishra, A.K. Sharma, Microwave–material interaction phenomena: heating mechanisms, challenges and opportunities in material processing, Compos.: Part A 81 (2016) 78–97, https://doi.org/10.1016/j.compositesa.2015.10.035.

[34] C. Leonelli, T.J. Mason, Microwave and ultrasonic processing: now a realistic option for industry, Chem. Eng. Process. 49 (2010) 885–900.

[35] Thomas Grosges, Alexandre Vial, Dominique Barchiesi, Models of near-field spectroscopic studies: comparison between Finite-Element and Finite-Difference methods, Opt. Express 13 (21) (2005) 8483–8497.

[36] QUICKWAVE, 2018. Software for electromagnetic design and simulations. From https://www.qwed.eu/QuickWave_2018.pdf.

[37] J.D. Gutiérrez-Cano, P. Plaza-González, A.J. Canós, B. García-Baños, J.M. Catalá-Civera, F.L. Peñaranda-Foix, A new stand-alone microwave instrument for measuring the complex permittivity of materials at microwave frequencies, IEEE Trans. on Instrum. and Meas. 69 (6) (2020) 3595–3605, https://doi.org/10.1109/TIM.2019.2941038.

[38] Felipe L. Peñaranda-Foix, Michael D. Janezic, Jose M. Catalá-Civera, Antoni J. Canós, Full-wave analysis of dielectric-loaded cylindrical waveguides and cavities using a new four-port ring network, IEEE Trans. Microw. Theory Tech. 60 (9) (2012) 2730–2740.

[39] S.K. Pathak, F. Liu, J. Tang, Finite difference time domain (FDTD) characterization of a single mode applicator, J. Microw. Power Electromagn. Energy 38 (2003) 37–48.

[40] Benoit Cosson, Fabrice Schmidt, Yannick Le Maoult, Maxime Bordival, Infrared heating stage simulation of semi-transparent media (PET) using ray tracing method, Int. J. Mater. Form 4 (1) (2011) 1–10, https://doi.org/10.1007/s12289-010-0985-8.